INDIAN INSTITUTE OF TECHNOLOGY,ROPAR

CAPSTONE PROJECT-I REPORT
ON

"DEVELOPMENT OF AI TOOL FOR THE DETECTION OF MINES USING GPR "

Submitted by

LOHIT SUBODH	**2017MEB1219**
NEERAJ PENUMAKA	**2017MEB1227**
JASHAN SANGER	**2017MEB1214**
MAYANK KESHARI	**2017MEB1220**

UNDER THE GUIDANCE OF
Dr.Manish Agrawal & Dr.Srikant Padhee

DEPARTMENT OF MECHANICAL ENGINEERING
IIT ROPAR
RUPNAGAR, PUNJAB - 140001

2020-2021

Submission Date:20 Dec,2020

Acknowledgements

We are profoundly grateful to **Dr. Manish Agrawal** and **Dr. Srikant Padhee** for his expert guidance and continuous encouragement throughout to see that this project rights its target since its commencement to its completion.

We would like to express deepest appreciation towards **Dr. Sarit K. Das**, Director, IIT ROPAR, **Dr. Ekta Singla**, Head of Department of Mechanical Engineering and **Dr. Manish Agrawal**, our Faculty Advisor for providing us with this opportunity.

At last we must express our sincere heartfelt gratitude to all the staff members of Mechanical Engineering Department who helped us directly or indirectly during this course of work.

LOHIT SUBODH
NEERAJ PENUMAKA
JASHAN SANGER
MAYANK KESHARI

Contents

List of Figures

Chapter 1

Introduction

Wars claim enough human lives, not only when parties are involved in it, but also years after it has ended. Innumerous numbers of mines are left astray around the war zone and pose as a threat to the civilian population around. Not only civilians but a good number of our soldier have lost their lives to these mines trying to find and neutralize them. According to the landmine monitor report 2018, at least 2793 people were killed and 4431 were injured in the year 2017. Among these 87% were civilian and around 47% were children. The largest numbers of casualties were in Afghanistan (2,300), Syria (1,906), and Ukraine (429). If their threat was not dangerous enough, with the advancement in technology over the years, the modern warfare has made way for non metallic mines that cannot be detected by using the traditional metal detectors. Since these cannot be caught using metal detectors, these pose even greater threat. This call for a new technology to be developed that can be used to detect these mines.

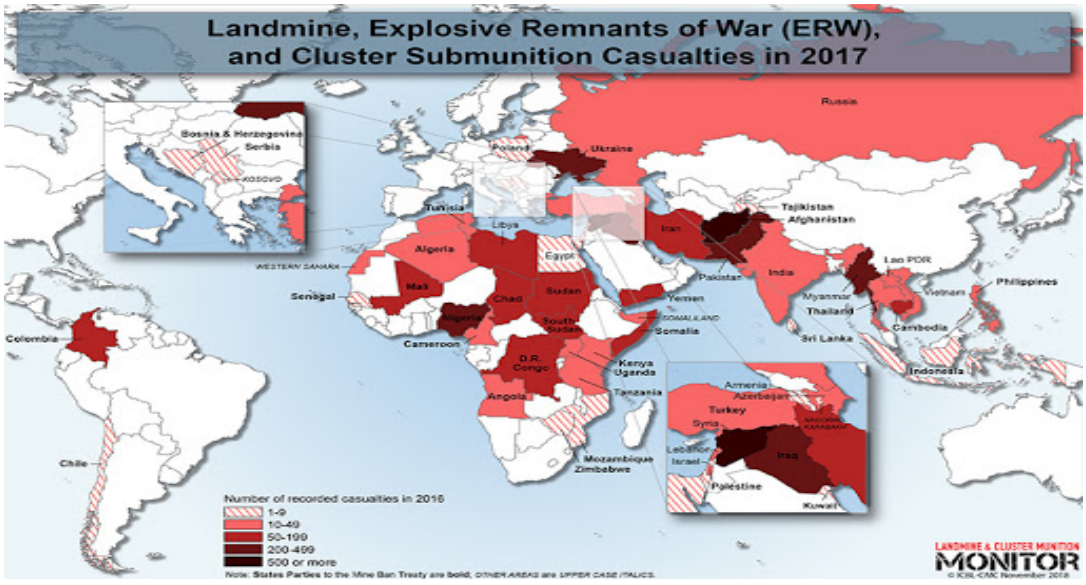

Figure 1.1: Landmines, EWR and cluster sub-munition casualties around the world - landmine moniter report 2018

In this project, we are trying to develop an AI tool based upon the GPR, with which we will be able to not only detect but localize that mine for a given region. The GPR technology uses electromagnetic radiations to detect underground objects based upon the electromagnetic responses from the surface. The GPR can detect the underground object but the real difficult is to verify whether it is actually a mine or not as GPR will detect any object like some old metal pipes or large rocks. Also, as the GPR is based upon electromagnetic radiation that behave differently in different materials, the difficulty of the task increases as we need to accommodate hot sands of the Thar desert and the snow covered land of the Himalayas into the tool. There are a lot of factors and parameters that need to be optimized.

The idea revolves around implementing a convolution neural network (CNN) upon the data obtained by the GPR. The data required for initial training and testing of the network, is obtained by running various simulations on the gprMax software, in which we can design a subsurface according to our needs and get the data that a GPR must have given for that kind of scenario. Data is generated for different kinds of terrains with and without mines and is used to train the model.

Chapter 2

Theoretical knowledge

2.1 Basics of GPR

The Ground Penetration Radar (GPR) technology is based upon the behavior of electro-magnetic waves at the intersection of different medium. GPR is used to get an image of the subsurface at a particular area. GPR is used to analyze various subsurface utilities like underground pipes, electrical transmission lines, concrete layers. It can also be deployed in various kinds of environments ranging from ice to rocks. Due to its versatile nature, the GPR technology is quite famous among people studying subsurface entities.

A typical GPR system has three main components: the transmitter, the receiver and the control unit. The transmitter, transmits an electromagnetic wave into the surface, the wave travels through the surface and deep in the subsurface getting reflected from various objects and at junctions of different mediums. The receiver collects the reflected rays that travel back after hitting an object or witnessing an intersection. The control unit evaluates the received and the transmitted waves and develops an image of the subsurface. The EM waves used for GPR broadly lies in the microwave band (UHF/VHF) with the frequency of the wave ranging from 30 MHz - 3 GHz. The frequency closer to 1 GHz can be found in most of the applications. The frequency of the wave plays very crucial roles. How deep we can go into the surface, how accurately can we identify the location and size of the object, the answer to these questions depends upon the frequency of the wave.

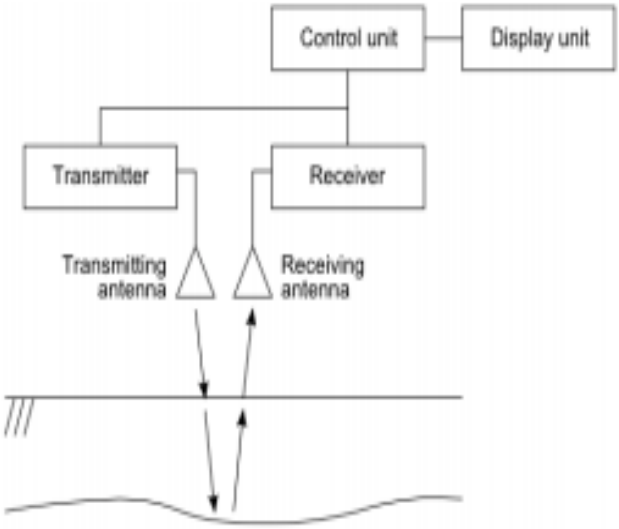

Figure 2.1: Block diagram of a GPR system

2.2 Electromagnetic principles of GPR

2.2.1 Wave Velocity

It is very essential to understand the propagation of an electromagnetic wave. EM waves travel at different speed in different mediums. Velocity of a wave in a particular medium depends upon the physical properties of the medium. The velocity of a wave in medium can be given by:

$$V = \sqrt{\frac{2}{\mu\varepsilon}}\left[\left(1+\left(\frac{\sigma}{\omega\varepsilon}\right)^2\right)^{1/2}+1\right]^{-1/2}$$

Where μ is the permeability of the medium, ε is the permittivity of the medium, σ is the electrical conductivity of the medium and ω is the frequency of the wave.

Considering the high frequency range in the GPR applications, $\sigma << \omega\varepsilon$. Therefore, the velocity can be given by:

$$V = \frac{1}{\sqrt{\mu\varepsilon}} = \frac{c}{\sqrt{\mu_r\varepsilon_r}}$$

Using this formula, we can easily find out the velocity of the wave in different mediums. For a non-magnetic material, the relative permeability can be considered equal to 1. For most of the soil material we can make this assumption and the velocity of the wave only depends upon the relative permittivity of the medium.

2.2.2 Reflection and Transmission of waves

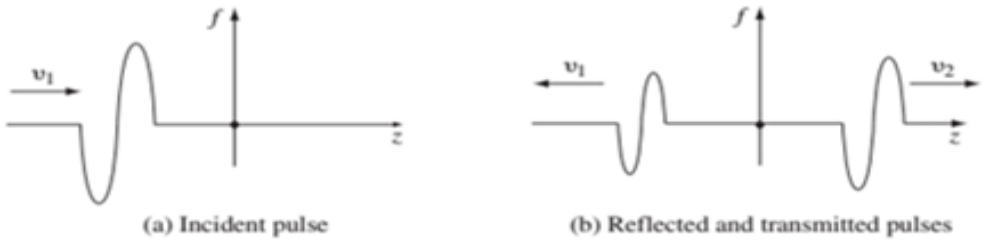

Figure 2.2: Reflection and transmission at an interface

When an EM wave encounter a change in the permittivity due to presence of an object in its path or due to the change of soil layer, some part of the wave energy gets reflected back and some is transmitted to the new medium. The reflection coefficient and the transmission coefficient are used to find the proportions of the wave amplitude that has been reflected and propagated through respectively. The simplest scenario is the case of a planar boundary with the wave incident perpendicular to the boundary. The reflection coefficient and the transmission coefficient for this scenario are given by:

$$R = \frac{\text{Reflected Amplitude}}{\text{Incident Amplitude}} = \frac{\sqrt{\varepsilon_1} - \sqrt{\varepsilon_2}}{\sqrt{\varepsilon_1} + \sqrt{\varepsilon_2}} \qquad T = \frac{\text{Transmitted Amplitude}}{\text{Incident Amplitude}} = \frac{2\sqrt{\varepsilon_2}}{\sqrt{\varepsilon_1} + \sqrt{\varepsilon_2}}$$

From the formula for R, we can see that if $\varepsilon 1 < \varepsilon 2$, then the value of R is less than zero and we can witness a reverse in polarity of the reflected wave. On the other hand, if $\varepsilon 1 > \varepsilon 2$, then there is no reverse I polarity of the reflected wave. If the $\varepsilon 1$ is similar to $\varepsilon 2$, most of the wave gets transmitted through the interface.

In case of a highly conductive object, these formulas do not hold up as the reflective and transmitted waves cannot be characterized by dielectric permittivity only. Consider the initial velocity equation for a wave. We can see that if the conductivity of the material is high the value of the velocity tends to be 0. So, if a highly conduc-

tive object is encountered in the subsurface the wave is completely reflected back regardless of the permittivity and the angle of incidence.

2.2.3 Propagation Losses

As the wave travels through various mediums and around different objects, there are a lot of factors that contribute to the loss of energy of the wave. It is very important to study these losses in order to estimate the amount of initial energy to be given to the pulse for it to reach till a particular depth into the soil. The total loss in energy in can be depicted as:

$$L_T = L_e + L_m + L_{t1} + L_{t2} + L_s + L_a + L_{sc}$$

where,

L_e = antenna efficiency loss in dB
L_m = antenna mismatch losses in dB
L_{t1} = transmission loss from air to material in dB
L_{t2} = retransmission loss from material to air in dB
L_s = antenna spreading losses in dB
L_a = attenuation loss of material in dB
L_{sc} = target scattering loss in dB

Among these losses, attenuation loss is the major contributor to the total loss. The antenna efficiency loss and antenna mismatch loss are specific to a particular system being used and the values for these losses are provided. The value of transmission loss from air to the soil material can be calculated but tabulated values for various soil materials are available and can be readily used. The antenna spreading loss is due to the spreading of the wave on a large area as we go deep into the soil. Target scattering loss is due to the scattering of the wave around the corners of the target or due to unwanted clutter present in the soil with dimensions comparable to the wavelength of the wave.

Attenuation loss is due to the continuous decrease in the amplitude of the wave as it propagates through the soil. The following formula can be used to get the amplitude of the wave at a particular depth ‘z’:

$$\frac{|\mathbf{A}|}{|\mathbf{A_0}|} = e^{-\alpha z}$$

Where α is the attenuation constant and is calculated using the following formula:

$$\alpha = \omega\sqrt{\frac{\mu\varepsilon}{2}}\left[\left(1+\left(\frac{\sigma}{\omega\varepsilon}\right)^2\right)^{1/2} - 1\right]^{1/2} \approx \begin{cases} \sqrt{\dfrac{\omega\mu\sigma}{2}} & \text{for } \omega\varepsilon \ll \sigma \\ \dfrac{\sigma}{2}\sqrt{\dfrac{\mu}{\varepsilon}} & \text{for } \sigma \ll \omega\varepsilon \end{cases}$$

For different frequencies of wave and various soil type tabulated data is available for the attenuation loss. Considering all the above described losses, one can estimate the amount of energy required for the pulse to be release by the transmitter of the GPR system.

2.3 Resolution and Probing Distance

Resolution can be defined as how accurately can we locate the position of the object in the ground. It can be further divided into accuracy in depth measurement and accuracy in size. Generally speaking, higher frequency waves give better resolution because they can detect the finest of details. But there are also higher chances that the wave will interact with the clutter in the soil, resulting in high levels of noise on the receiver.

Resolution can be further divided into horizontal and vertical resolution. Horizontal resolution is the minimum distance between 2 objects for them to be detected. If the distance between 2 objects is less than the horizontal resolution then it will be detected as one. Vertical resolution, on the other hand is the minimum thickness of the object in the vertical direction for the object to be detected. If the thickness is less then vertical resolution then the object will not be detected.

The following formula can be used to get horizontal resolution:

$$Hr = \frac{c}{4 \cdot f \cdot \sqrt{RDP}} + \frac{D}{\sqrt{RDP+1}} \quad (2)$$

where:

Hr is the horizontal resolution

c is the speed of light in vacuum

f is the center frequency of the antenna

RDP is the relative dielectric permittivity

D is the depth to the plane where the two objects are located.

The following formula can be used to get vertical resolution:

$$Vr = \frac{Tpulse \cdot c}{2 \cdot \sqrt{RDP}} \quad (1)$$

where:

Vr is the vertical resolution

Tpulse is the transmitted pulse duration, this can be calculated by taking the inversion of the fundamental or center frequency.

c is the speed of light in vacuum

RDP is the relative dielectric permittivity of the media.

The probing distance is an estimate of the maximum depth that can be reached using a GPR system. To calculate the actual depth that the system can reach we have to consider all the losses discussed earlier for different depths and find out whether a particular depth is feasible for a system or not. This is a very time consuming process and thus to get an approximation of the maximum depth achievable, probing distance is considered as 3 times the value of the skin depth. Skin depth is the distance after which the amplitude of the wave reduces by a factor of 1/e. The following formula is used to get the value of the probing distance:

$$D = 3\delta \approx \begin{cases} 1510\sqrt{\dfrac{1}{\sigma f}} & \text{for } \omega\varepsilon \ll \sigma \\ 0.0159\dfrac{\sqrt{\varepsilon_r}}{\sigma} & \text{for } \omega\varepsilon \gg \sigma \end{cases}$$

Data related to probing distance for different soil types and various frequencies is available and can be used directly. The following graph shows the relationship between probing distance and the frequency of the wave for different soil type:

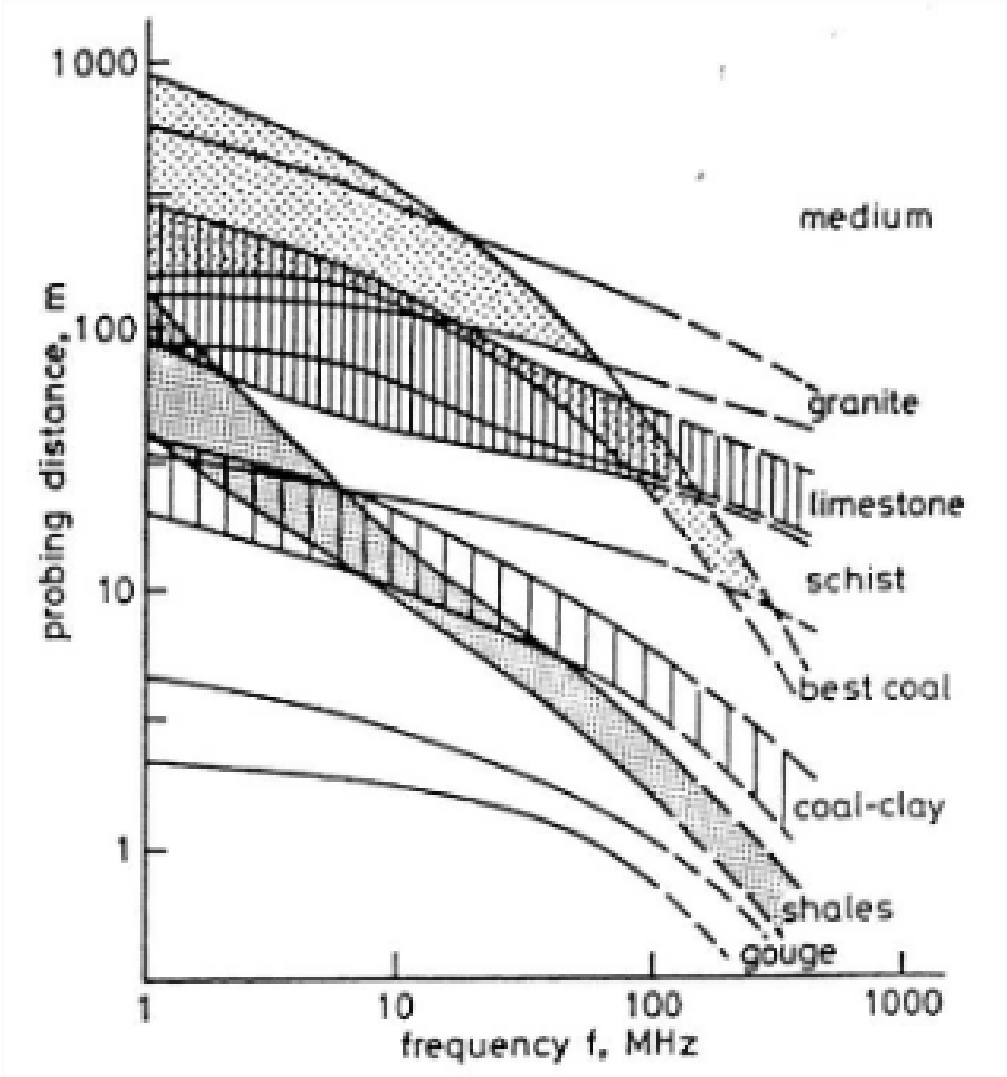

Figure 2.3: Probing distance for various materials from 1 MHz to 1 GHz

Chapter 3

gprMax(Simulation software) Basics

3.1 Generating B-scan

gprMax is open-source software that simulates electromagnetic wave propagation. It solves Maxwell's equations in 3D using the Finite-Difference Time-Domain (FDTD) method. It is designed for simulating Ground Penetrating Radar (GPR) and can be used to model electromagnetic wave propagation in fields such as engineering, geophysics, archaeology, and medicine. gprMax is command-line-driven software written in Python with performance-critical parts written in Cython. As there is no graphical user interface for this software, we used ParaView software to visualize our model's geometry.

One of the most challenging issues in modeling open boundary problems, such as GPR, is the truncation of the computational domain at a finite distance from sources and targets where the electromagnetic fields' values can not be calculated directly by the numerical method applied inside the model. Hence, an approximate condition known as an absorbing boundary condition (ABC) is used at a sufficient distance from the source to truncate and limit the computational space. This ABC's role is to absorb any waves impinging on it, hence simulating an unbounded space.

Consider a metal cylinder buried in a dielectric half-space.The geometry of the scenario is shown in Fig3.1. Fig3.2 shows the time history of the electric and magnetic field components and currents at the receiver location. The Ez field component can be converted to voltage which represents the A-scan

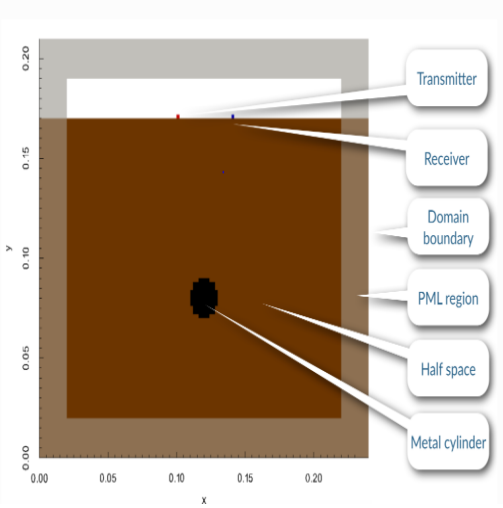

Figure 3.1: Cylinder buried in a dielectric half-space

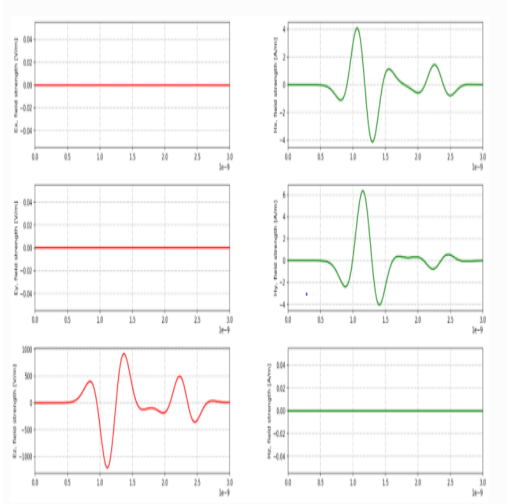

Figure 3.2: Electric and magnetic field components

A B-scan is composed of multiple traces (A-scans) recorded as the source and receiver are moved over the target, in this case the metal cylinder.

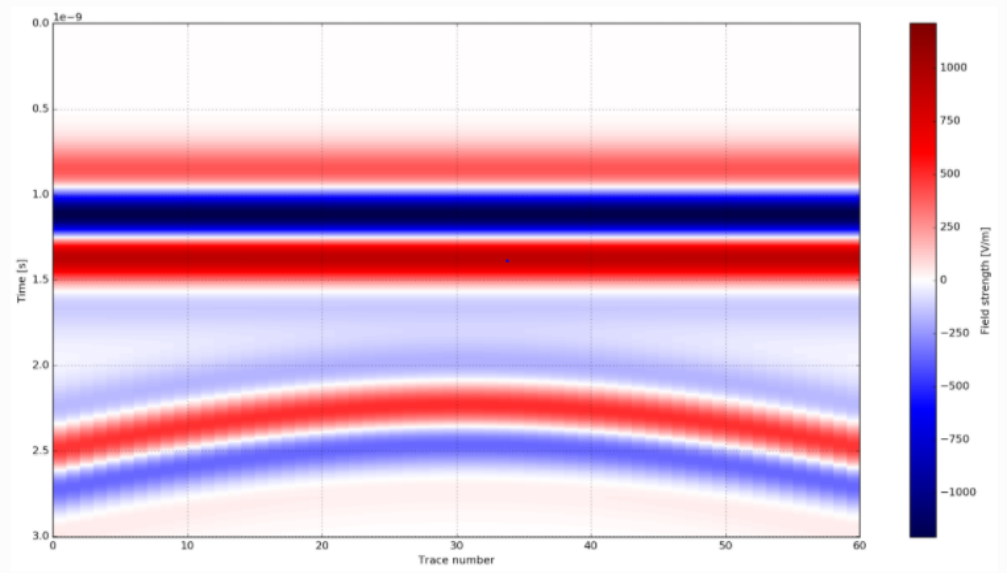

Figure 3.3: B-scan of metal cylinder buried in a dielectric half-space.

3.2 Domain Discretization

gprMax allows us to specify the discretization of space in the x, y and z directions respectively (i.e., Δx, Δy, Δz). The spatial discretization controls the maximum permissible time step Δt with which the solution advances in time in order to reach the required simulated time window. The relation between Δt and Δx, Δy, Δz is:

$$\Delta t \leq \frac{1}{c\sqrt{\frac{1}{(\Delta x)^2}+\frac{1}{(\Delta y)^2}+\frac{1}{(\Delta z)^2}}},$$

where c is the speed of light. In gprMax the equality is used to determine Δt from Δx, Δy and Δz. Small values of Δx, Δy and Δz result in small values for Δt which means more iterations in order to reach a given simulated time. However, the smaller values of Δx, Δy, Δz and Δt result in an accurate model.

In the input file of gprMax, we mention all the details of our model. According to our requirement, we can vary the environment parameters such as domain size, surface roughness, soil constituents, moisture content, vegetation, surface water, etc. The antennas' position and the location of the mine should also be given as an input parameter. An example of the input file is shown in the figure 3.4.

```
#title: Water Puddles
#domain: 1.0 0.25 0.45
#dx_dy_dz: 0.001 0.001 0.001
#time_window: 6e-9

#python:
from user_libs.antennas.GSSI import antenna_like_GSSI_1500
antenna_like_GSSI_1500(0.1 + current_model_run * 0.006, 0.126,0.24,0.001)
#end_python:

#soil_peplinski: 0.5 0.5 2.0 2.66 0.001 0.25 my_soil
#fractal_box: 0 0 0 1.0 0.25 0.2 1.5 1 1 1 50 my_soil my_soil_box
#add_surface_roughness: 0 0 0.2 1.0 0.25 0.2 1.5 1 1 0.195 0.205 my_soil_box
#add_surface_water: 0 0 0.2 1.0 0.25 0.2 0.203 my_soil_box

#material: 3.5 0.01 1.0 0 bakelite
#material: 6.0 0.01 1.0 0 rubber
#material: 2.86 0.00048 1.0 9.75 TNT
#material: 2.4 0 1 0 plastic

        PMN
#cylinder: 0.3 0.126 0.15 0.3 0.126 0.147 0.056 rubber
#cylinder: 0.3 0.126 0.147 0.3 0.126 0.094 0.056 bakelite
#cylinder: 0.3 0.126 0.147 0.3 0.126 0.097 0.053 TNT
#cylinder: 0.3 0.126 0.147 0.3 0.126 0.097 0.002 pec

        PMA-1
#box: 0.65 0.09 0.12 0.79 0.16 0.15 plastic
#box: 0.67 0.10 0.13 0.77 0.15 0.14 TNT
#cylinder: 0.67 0.12 0.135 0.77 0.12 0.135 0.002 pec
```

Figure 3.4: Input File

3.3 Model Visualization

Our model's geometry file (which is in .vti format) is generated using the input file. This geometry file helps in the model visualization using the ParaView software.

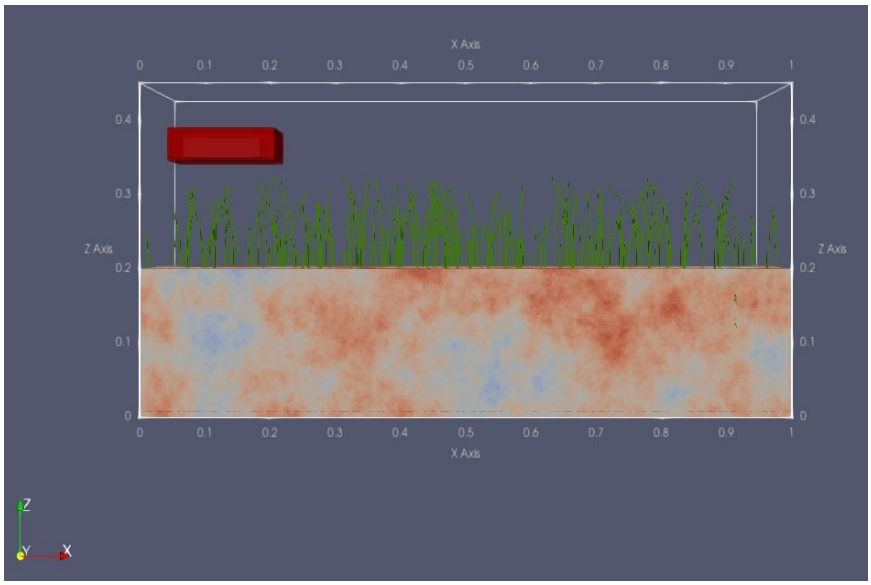

Figure 3.5: Simulation environment (the red box indicates the antennas i.e., transmitter and receiver)

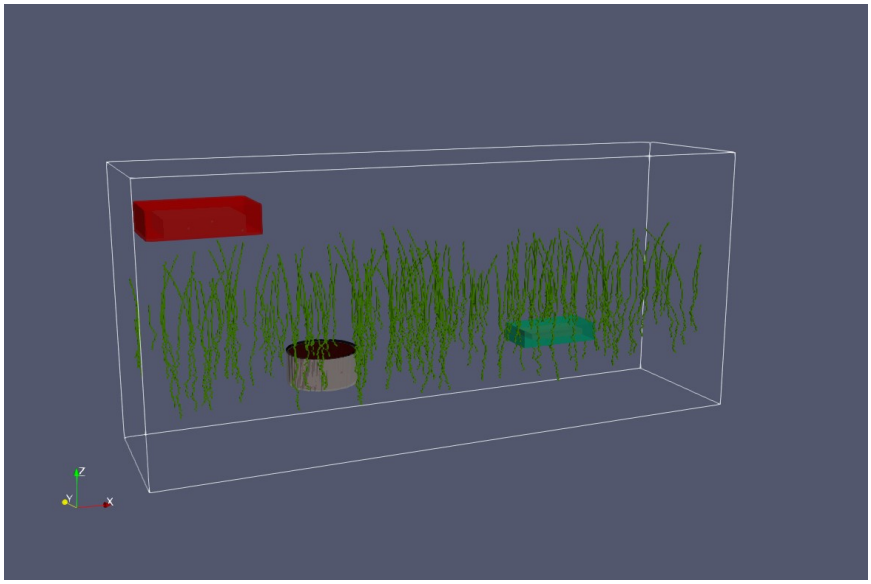

Figure 3.6: PMN and PMA-1 mines (soil opacity is reduced to zero for better visualisation)

Chapter 4

Data Generation using gprMax

The input files are generated using Python scripting. Random values of various parameters like surface roughness, soil constituents, and height of vegetation are generated using Python's inbuilt distribution functions. The domain size, spatial step, and time window are fixed. The ratio of input files with mine to that of without mine is 20:80. PMN mine is considered in the case of input files with mine. The model is run 60 times to get the complete B-scan, with the antenna moving with a step size of 5 mm in each run. The figure 4.1 shows the parameters that are varied for various data points.

Sl. No.	Sand Fraction	Clay Fraction	Bulk Density (g/cc)	Sandparticle Density (g/cc)	Water Fraction	Surface Roughness (lower limit)	Surface Roughness (higher limit)	Height of Vegetation (lower Limit)	Height of Vegetation (higher limit)
1	0.412	0.588	2.018	2.682	0.103	0.235	0.267	0.269	0.296
2	0.308	0.692	2.038	2.8	0.094	0.233	0.281	0.254	0.298
3	0.403	0.597	1.952	2.706	0.177	0.23	0.267	0.27	0.296
4	0.395	0.605	1.849	2.685	0.244	0.226	0.251	0.264	0.294
5	0.376	0.624	2.184	2.633	0.122	0.234	0.265	0.255	0.297
6	0.354	0.646	2.184	2.747	0.24	0.202	0.266	0.263	0.292
7	0.378	0.622	2.016	2.504	0.134	0.249	0.261	0.251	0.291
8	0.39	0.61	2.366	2.565	0.079	0.22	0.259	0.251	0.3
9	0.387	0.613	1.894	2.631	0.16	0.213	0.284	0.265	0.298
10	0.524	0.476	1.897	2.616	0.24	0.237	0.278	0.267	0.293

Figure 4.1: A sample of 10 Data Points (the values of the surface roughness and vegetation are the spatial height coordinates, with 0.25 being the value for zero roughness and no vegetation)

```
#title: mine1
#domain: 0.5 0.25 0.45
#dx_dy_dz: 0.002 0.002 0.002
#time_window: 5e-9

#python:
from user_libs.antennas.GSSI import antenna_like_GSSI_1500
antenna_like_GSSI_1500(0.1 + current_model_run * 0.005, 0.126,0.30,0.002)
#end_python:

#soil_peplinski: 0.412 0.588 2.018 2.682 0.05299999999999999 0.103 my_soil
#fractal_box: 0 0 0 0.5 0.25 0.25 1.5 1 1 1 50 my_soil my_soil_box
#add_surface_roughness: 0 0 0.25 0.5 0.25 0.25 1.5 1 1 0.235 0.267 my_soil_box

#add_grass: 0 0 0.25 0.5 0.25 0.25 1.5 0.269 0.296 200 my_soil_box

    PMN mine
#material: 3.5 0.01 1.0 0 bakelite
#material: 6.0 0.01 1.0 0 rubber
#material: 2.86 0.00048 1.0 9.75 TNT
#material: 2.4 0 1 0 plastic

#cylinder: 0.25 0.126 0.20 0.25 0.126 0.197 0.056 rubber
#cylinder: 0.25 0.126 0.197 0.25 0.126 0.144 0.056 bakelite
#cylinder: 0.25 0.126 0.197 0.25 0.126 0.147 0.053 TNT
#cylinder: 0.25 0.126 0.197 0.25 0.126 0.147 0.002 pec
```

Figure 4.2: Input file for the first data point in the figure 4.1

After generating the input files, the next step is to run all the input files using gprMax and store the B-scan data. For this step, we used a simple shell script to automate the process. This labelled B-scan data is then fed into a machine learning model which helps in predicting the probability of presence of a landmine.

Chapter 5

CNN model

We have used CNN architecture as our model. CNN's or Convolutional neural network are best known for their ability to recognize patterns present in images. As we have to predict whether the given B-scan obtained from simulation contains a mine or not, which is an image classification task, we choose CNN.

A CNN has basically consists of these layers:
1) Fully connected: layers performing dot product between the input and a parametric matrix.
2) Convolutional: layers applying multidimensional convolution to the input.
3) Activation: layers applying a nonlinear operation (e.g., hyperbolic tangent, rectification, etc.) to the input.
4) Pooling: layers processing the input with a moving window, and outputting a selection of the samples within each window (e.g., the maximum, minimum, average, etc.).

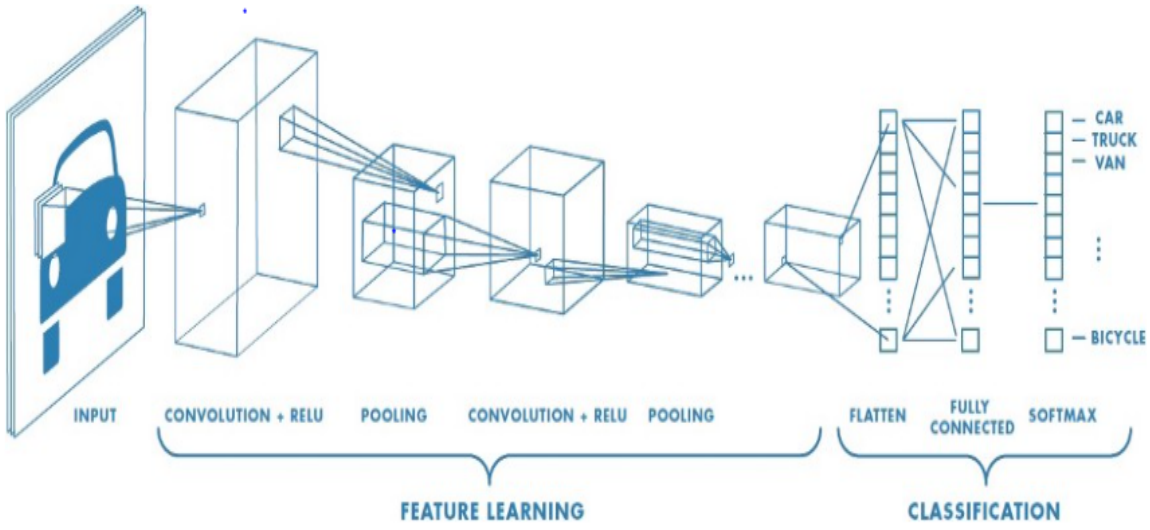

Figure 5.1: CNN Architecture

Fig5.1 shows the architecture of a general CNN used for image classification problem. We have tried several architecture and found the best architecture for our problem which gives best accuracy. Our CNN architecture is composed of the following.
1) One 2-D convolutional layer with 20 filters, stride 1×1, size 5 × 5.
2) Max Pooling layer with size 2 x 2.
3) 2-D convolutional layer with 50 filters of size 5 x 5.
4) Max Pooling layer with size 2 x 2.
5) 2-D convolutional layer with 500 filters of size 4 x 4 and relu activation.
6) Dropout with 0.5 probability.
7) Max Pooling layer with size 2 x 2.
8) 2-D convolutional layer with 26 filters of size 2 x 1.
9) Flatten the vector and add Dense layer with activation softmax.
Fig5.2 shows our model summary. Total trainable parameters are 705,598.

```
Model: "sequential"
_________________________________________________________________
Layer (type)                 Output Shape              Param #
=================================================================
conv2d (Conv2D)              (None, 1300, 60, 20)      520
_________________________________________________________________
max_pooling2d (MaxPooling2D) (None, 650, 30, 20)       0
_________________________________________________________________
conv2d_1 (Conv2D)            (None, 650, 30, 50)       25050
_________________________________________________________________
max_pooling2d_1 (MaxPooling2 (None, 325, 15, 50)       0
_________________________________________________________________
conv2d_2 (Conv2D)            (None, 325, 15, 500)      400500
_________________________________________________________________
dropout (Dropout)            (None, 325, 15, 500)      0
_________________________________________________________________
conv2d_3 (Conv2D)            (None, 325, 15, 26)       26026
_________________________________________________________________
flatten (Flatten)            (None, 126750)            0
_________________________________________________________________
dense (Dense)                (None, 2)                 253502
=================================================================
Total params: 705,598
Trainable params: 705,598
Non-trainable params: 0
```

Figure 5.2: CNN model summary

Several optimizers are tested for training such as Adam,SGD,RMSprop etc. Found SGD performs better than others. Learning rate = $1e^{-4}$ with momentum = 0.9 is used. Loss for our model is categorical crossentropy. Metrics is accuracy. Softmax activation is used in output layer to give probability of each class as the result. We ran our model for 10 epochs with a batch size of 100.

Chapter 6

Results and Observations

We have developed a CNN model which is able to detect the presence or absence of landmine. The data used for training the model is generated using gprMax software, and is almost similar to the real life data.

To study the effect of change in size of spatial discretization in gprMax, the simulated data generated using both 1 mm and 2 mm discretization size is observed. Although the results using the 1mm are more accurate, data generation using 1 mm discretization requires a great deal of computational power and an ample amount of time. In the 2 mm case, the results slightly deviate, but the advantage of less computational power outweighs the inaccuracy. So, the domain discretization is 2 mm (considering our resources) for all the simulations.

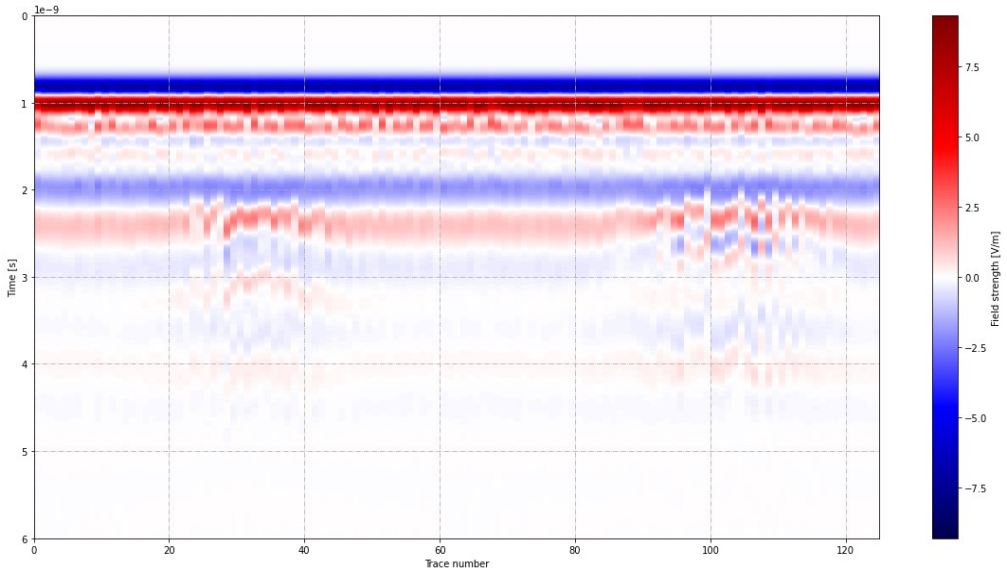

Figure 6.1: B-scan (using Δx = 1 mm)

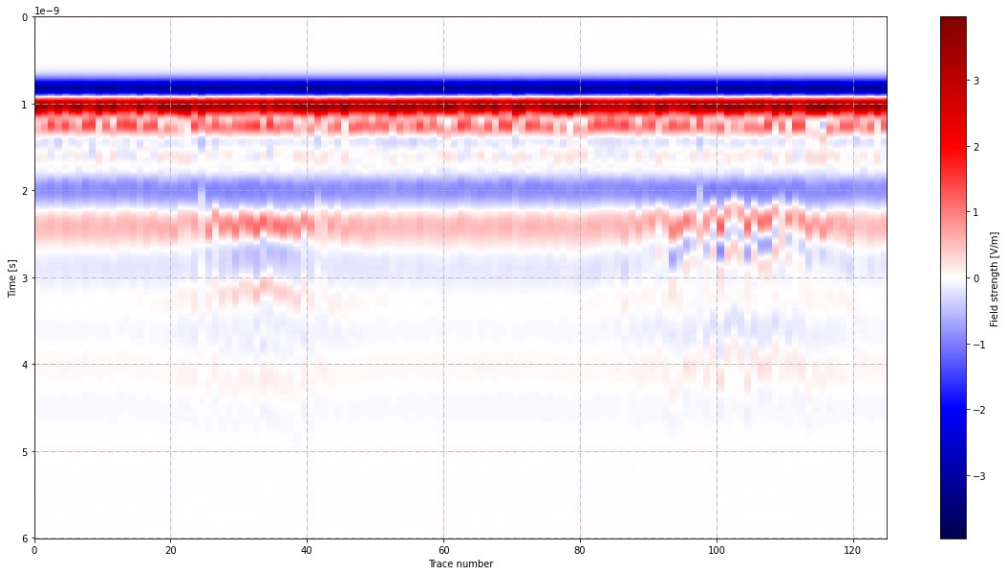

Figure 6.2: B-scan (using Δx = 2 mm)

The labelled B-scan data obtained after simulating the input files is fed into the CNN model. This labelled data is first split into training and testing data. The test data constitutes about 33% of the total data set. This part of the data is not seen by the learning algorithm. The learning is entirely done using the training data. The model tries to decrease the cost function based our training data. We generally refer to this value as loss, which indicates the penalty for failing to achieve a desired value. The desired value of loss should be close to zero. Figures 6.3 and 6.4 depict the loss vs number of epochs and accuracy vs number of epochs.

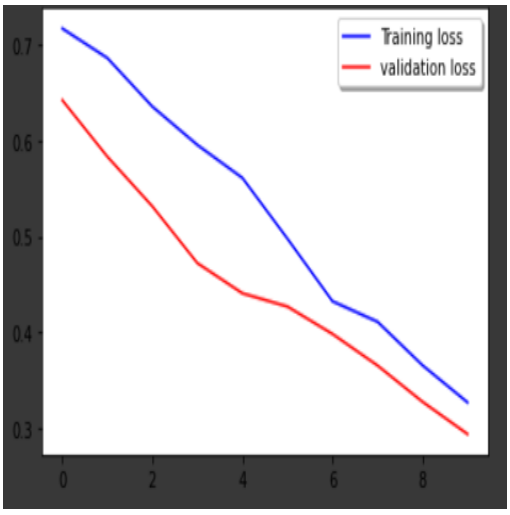

Figure 6.3: Loss vs number of epochs

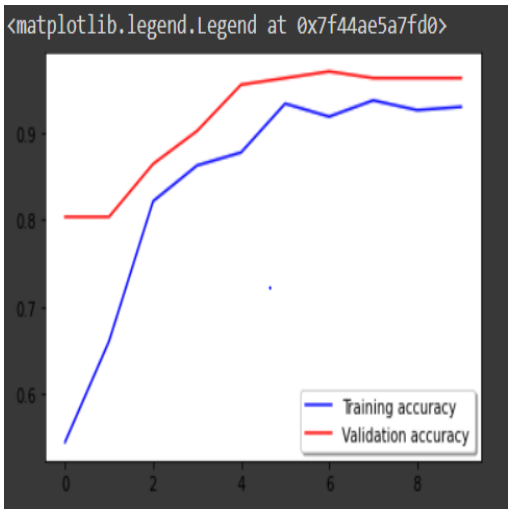

Figure 6.4: Accuracy vs number of epochs

As we can see from the above figures, loss decreases as we keep on increasing the epochs, also the accuracy increases with the number of epochs both for the training

and the validation data. We have trained our model for few epochs to avoid overfitting. After certain number of epochs accuracy reaches saturation and becomes difficult to increase. Our CNN model shows a accuracy of **96.21%** and loss of **0.293** on test dataset which consists of 132 B-scan images. As the test data is unseen by the model, it can even be tested on real life data and can achieve high accuracy.

We have also plotted confusion matrix to get a better understanding of our results.Fig 6.3 shows confusion matrix for the test dataset. Out of 103 images without mine, our model classifies 102 images correctly. Also 25 images are classified correctly for with mine out of 29 images. False negative (i.e., image with mine classified as without mine) of our model is 1 which is too low and desired as well.

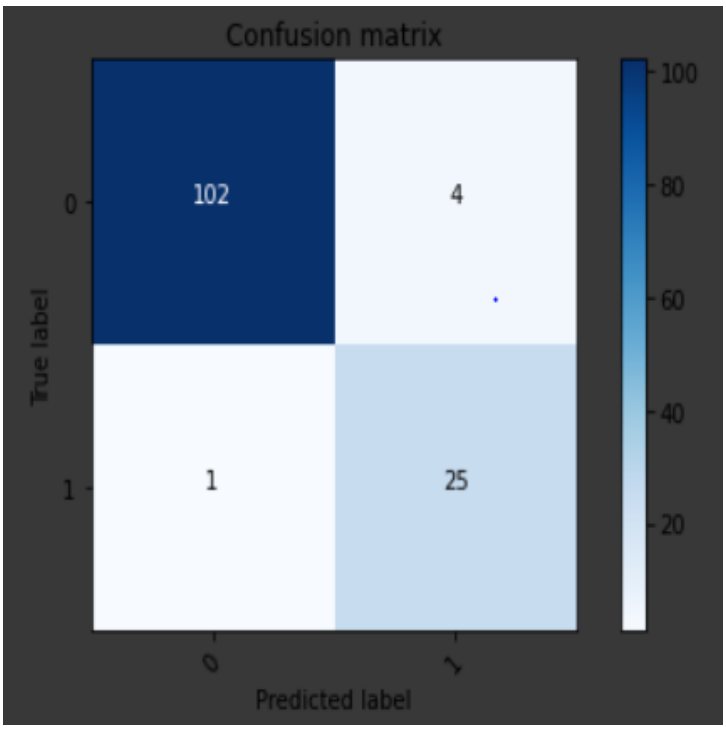

Figure 6.5: Confusion matrix for test data

Note: Google Colab notebook which contains code written in python for detecting mines can be accessed from here

Chapter 7

Conclusion and Future Work

In this report, a novel technique for landmine detection using gpr has been introduced. The proposed system is able to detect mines with the accuracy of 91.2% . Also the false negative is very low which is desired. The data used for training has been generated by using gprMax software to replicate real life conditions.The training data set used is very small (i.e., around 400 B-scans) and the convergence of the training is reached after a few epochs (i.e., a few minutes on a modern GPU). The proposed architecture can be trained on any data set and then refined on the area of investigation, whose conditions may vary everyday due to change in weather conditions and other external causes. Our model learns the patterns formed by hyperbolas in B-scans.

We can improve the performance of our model by further increasing the size of the dataset. Applying data augmentation can make our model more robust and prevent overfitting. The model is not yet tested on real-life data, but the model is also expected to perform better in those conditions. Currently, the model is trained to perform only the classification task. We can further develop the model to perform the tasks such as calculating the depth of the mine from the surface. Unsupervised learning techniques can also be applied to train the model(i.e., our model is trained with no pre-existing labels and with minimum human supervision). We can also use other machine learning algorithms such as ANN, SVM, KNN, Random Forest, auto-encoder, etc. to improve model performance.

References

[1] *M. Pham and S. Lefèvre, "Buried Object Detection from B-Scan Ground Penetrating Radar Data Using Faster-RCNN," IGARSS 2018 - 2018 IEEE International Geoscience and Remote Sensing Symposium, Valencia, 2018, pp. 6804-6807, doi: 10.1109/IGARSS.2018.8517683.*

[2] *Numerical modelling and neural networks for landmine detection using ground penetrating radar 2015 8th International Workshop on Advanced Ground Penetrating Radar (IWAGPR) Published: 2015*

[3] *S. Lameri, F. Lombardi, P. Bestagini, M. Lualdi and S. Tubaro, "Landmine detection from GPR data using convolutional neural networks," 2017 25th European Signal Processing Conference (EUSIPCO), Kos, 2017, pp. 508-512, doi: 10.23919/EUSIPCO.2017.8081259.*

[4] *V. Kafedziski, S. Pecov and D. Tanevski, "Detection and Classification of Land Mines from Ground Penetrating Radar Data Using Faster R-CNN," 2018 26th Telecommunications Forum (TELFOR), Belgrade, 2018, pp. 1-4, doi: 10.1109/TELFOR.2018.8612117.*

[5] *F. Picetti, G. Testa, F. Lombardi, P. Bestagini, M. Lualdi and S. Tubaro, "Convolutional Autoencoder for Landmine Detection on GPR Scans," 2018 41st International Conference on Telecommunications and Signal Processing (TSP), Athens, 2018, pp. 1-4, doi: 10.1109/TSP.2018.8441206.*

[6] *http://docs.gprmax.com/en/latest/*

[7] *https://towardsdatascience.com/simple-introduction-to-convolutional-neural-networks-cdf8d3077bac*

[8] *https://www.sensoft.ca/blog/what-is-gpr/*

[9] *http://www.the-monitor.org/en-gb/reports/2018/landmine-monitor-2018.aspx*

[10] *https://www.intechopen.com/books/mine-action-the-research-experience-of-the-royal-military-academy-of-belgium/ground-penetrating-radar-for-close-in-mine-detection*

[11] *https://gpg.geosci.xyz/content/GPR/*